Eur. Phys. J. B **3**, 377–385 (1998)

THE EUROPEAN PHYSICAL JOURNAL B

Diffusive properties of motion on a bumpy plane

L. Samson[1,a], I. Ippolito[1], G.G. Batrouni[2,3], and J. Lemaitre[1]

[1] Groupe Matière Condensée et Matériaux, Campus de Beaulieu, Université de Rennes I, 35042 Rennes Cedex, France
[2] Institut Non-Linéaire de Nice, Université de Nice-Sophia Antipolis, 1361 route des Lucioles, 06560 Valbonne, France
[3] HLRZ, Forchungszentrum, 52425 Jülich, Germany

Received: 13 March 1997 / Revised: 10 December 1997 / Accepted: 17 February 1998

Abstract. We report on experiments studying the statistical properties of the motion of balls on a bumpy surface. This motion is found to be diffusive. In the direction of the mean flow, the coefficient of diffusion is found to attain a constant value, independent of the size of the ball and the inclination angle. The diffusion transverse to the mean flow is characterized by a coefficient which decreases with the inclination of the plane, and scales with the size of moving ball.

PACS. 05.20.-y Statistical mechanics – 64.60.-i General studies of phase transitions

1 Introduction

The past fifteen years have seen a rapid growth of interest in the behaviour of granular media due to their fascinating properties and wide range of applications in many industries. A major industrial problem is that of obtaining good mixtures of grains of various sizes and masses. This difficulty arises from the natural tendencies of granular systems to segregate due to various effects such as [1] convection [2–4], diffusion [5,6] and flow [7]. The understanding of these mechanisms can lead to more efficient mixing strategies.

In this paper, we study in detail the motion of balls on rough surfaces. This is an idealization of what takes place on top of flowing granular systems: the top layers of such systems can be regarded as rough surfaces (idealized to planes) on which grains of various sizes can flow. Our goal in studying these idealized systems is to understand the roles of flow and friction and shocks in segregation and mixing.

We first summarize some of the results of previous experiments done on this system [8,9]. Depending on the inclination angle, θ, of the rough surface with respect to the horizontal and the smoothness, $\Phi = R/r$ (R is the radius of the rolling ball and r is that of the surface beads) three types of behaviour are observed [8] which can be summarized by a "phase diagram" consisting of three regions, denoted (A), (B) and (C). Region (A) is the pinning region where the ball quickly comes to a stop regardless of its initial velocity. In regime (B) the ball reaches a steady state with a mean constant velocity, $\overline{V_x}$, which is independent of the initial velocity. Regime (C) corresponds to the zone where the ball moves down the plane with big bounces and does not reach a steady state on the two meter long plane. Experiments performed by Aguirre *et al.* [10] evidenced that the existence of these 3 regimes was independent of the type of rolling ball or surface bead materials. Moreover they have observed that boundaries between regimes, in the different phase diagrams, do not change qualitatively. In the above experimental studies [8, 10], it was found, in regime (B), that the average velocity of the ball scales with the smoothness, and that the friction force is viscous, *i.e.* the velocity is given by the equation

$$\frac{\overline{V_x}}{\sqrt{rg}} \propto \Phi^{\beta} \sin(\theta). \tag{1}$$

The exponent β was found equal to 1.5 in Riguidel's experiments and 1.4 in Aguirre's ones. However, the average velocity is not as a simple function of R/r as was previously thought. Even though the details are not known, the packing fraction does seem to play a role in determining the average velocity. A recent study [11] found β equal to 1.25 for a packing fraction of the surface of 0.67 which is smaller than those used in the previously mentioned studies. Of course, this difference is no longer surprising since one of our main conclusions is that the geometry of the system is of crucial importance. Using arguments like Bagnold's [12,13] one expects an effective frictional force proportional to V^2 which would give an average velocity proportional to $\sqrt{\sin(\theta)}$. Recently Batrouni *et al.* [14] presented a 1D stochastic model in which geometry plays a crucial role. This model reproduces most aspects of the motion of the ball on the rough inclined plane, including the viscous frictional force and the scaling with the smoothness. The agreement of this model with experiments emphasizes the important role played by the

[a] e-mail: liliane.samson@univ-rennes1.fr

geometry of the surface. In the particular case of region (B), the trajectory of a sphere on an inclined rough surface can be pictured as a driven random walk where the fluctuations of the local velocities are due to the collisions between the moving sphere and the surface grains. An interesting question is whether it is possible to find a characteristic length for the motion and, if so, what influence the roughness has on it. Molecular Dynamics simulations [15, 16] reproducing the motion of the ball on a rough line or a rough plane have been performed in parallel with our experiments. After presenting our experimental results, we will discuss and compare the two. The present study concentrates on the experimental characterization of the local geometrical parameters such as the roughness seen by a moving sphere and the inclination angle of the rough surface. This paper is organized as follows: the experimental techniques are described in Section 2. The experimental results are presented in Section 3 and discussed in Section 4.

2 Experimental setup

2.1 The rough surface

The experimental study of the diffusion of a single ball on a rough surface requires good geometrical control *i.e.* a rough surface which is quite disordered and homogeneous, and an accurately measured inclination angle. So we have built an experimental device which is quite similar to that used by Riguidel *et al.* [8,9]. The control parameters are the angle θ between the rough surface and the horizontal, and R, the radius of the steel ball which moves on the plane. r is the radius of the glass beads constituting the rough surface. We use a two meter long by one meter wide plane of 1 cm thick glass plate supported by a rigid metallic frame. The rough surface is made of glass beads of radius, r, close to (0.53 ± 0.03) mm stuck on adhesive plastic sheet. The size of these glass beads is kept constant for all experiments. This technique allows us to obtain a monolayer of beads which is disordered and roughly homogeneous. We have obtained a surface packing fraction of (0.67 ± 0.03). This was measured by counting the number of glass beads in 20 patches of equal area (4 cm^2). Typical ball diameters used in our experiments range between 2.5 and 7 mm. The launched balls are made of steel, with a density of 7.85 g/cm^3, and a well defined sphericity, with uncertainty less than 0.25 μm. The tolerance in the diameter of the balls is 10.25 μm. The balls are launched parallel to the rough surface by a mechanism consisting of a tap with a reservoir. A stepping motor is fixed on the tap in order to automate the launching. Each time the tap turns a half rotation, a ball is released while another enters in the tap. This system allows us to launch a large number of balls to obtain good statistics. The initial velocity of the ball (in magnitude and direction) before reaching the surface needs to be well controlled too. The balls do not fall directly on the rough plane, but first on a gutter, which allows control of the direction of the initial velocity. They arrive on the gutter with practically zero velocity. The length subsequently travelled on the gutter can be varied so the initial velocity can be modified. Generally, in our experiments, the distance travelled on the gutter is the same and close to 1 cm, the smallest length allowed by the setup, for all R and θ. So as θ increases, the initial velocity is also increased. Neglecting friction between the ball and the gutter, we estimate the typical initial velocity values to range between 9 to 34 cm/s, *i.e.* not far from the mean constant velocity values, except for $R = 1.25$ mm and $R = 1.5$ mm. In these two cases, the initial velocities are in fact close to 30 cm/s while the mean constant velocities are close to 7 cm/s, with the inclination angles for the regime (B) being between 7 and 9.5 degrees. But even if we study the regime (B), *i.e.* where the mean constant velocity is independent of the initial velocity, it is important to launch the ball with the same initial velocity because, before reaching the mean constant velocity regime, the ball has a transient motion, which can bias the dispersion measurements. This transient regime is shorter the closer the initial velocity is to the mean constant velocity.

2.2 Dispersion measurements

We used two experimental techniques to study ball diffusion on the rough surface in regime (B), *i.e.* the mean constant velocity zone. In the first experimental technique (for longitudinal and transverse dispersion measurements) the travelled distance is fixed, and the transit time distribution is measured to study the longitudinal dispersion. In the second one the time interval is fixed close to 1/25 seconds and the travelled distance is measured.

In order to study the transverse dispersion we have built a metallic collector with 70 bins of adjustable width, which is made slightly larger than the diameter of the balls used in the experiments. The walls dividing the bins are very thin in order not to bias the binning. The experimental setup for the transverse and longitudinal dispersion is shown in Figure 1. The distance, L, from the launcher to the collector can be changed. For a given distance L, a series of 200 balls are released for each of three different launching points. The different release positions serve to avoid having the particles take a preferential path caused by possible flatness problems or local imperfections in the 2D arrangements of the glass beads of the surface. In this way the balls reach the collector and enter into the different bins giving the corresponding distributions. The experimental setup for the longitudinal dispersion measurements is as follows. A range of 8 lasers [17] is placed along the length of the rough plane. A first laser beam is placed at the release position of the balls for triggering the timer. The remaining 7 lasers are ranged in the region of the plane where the ball attains its steady state. These lasers are separated by equal distances which are adjustable in units of 5 cm. Symmetrically a range of 8 phototransistors [18] is placed at the opposite side of the plane. The transit time of the ball is recorded when it crosses a laser beam. Finally the last beam is also used to initiate the launch of a new ball and so on. All measurements are controled by a computer giving us the transit time distributions of the

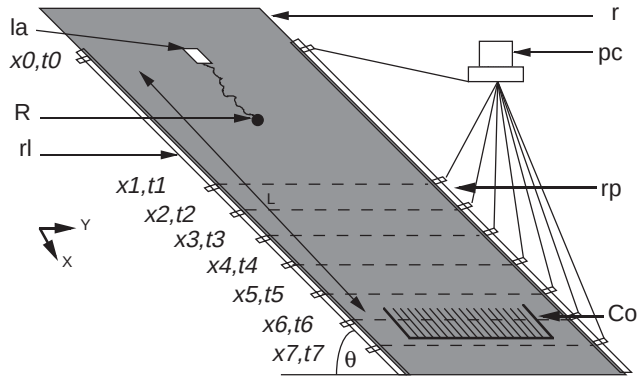

Fig. 1. Experimental setup for measuring transverse and longitudinal dispersion: (la) steel ball launcher, (R) ball radius R, (Co) collector, (L) distance between the launcher and the collector, (PC) Personal Computer, (rl) range of lasers, (rp) range of photodetectors, (r) glass beads radius constituting the rough surface, (θ) angle between the rough plane and the horizontal.

rolling balls. In regime (B) and for small angles θ some balls may get trapped [8] in which case these particles are not considered. These balls have the same dynamics as the ones which do not get trapped, so even if they are not taken into account there is no bias in the statistics. For a given angle θ and radius R, a thousand balls are launched. The uncertainty in the time is less than $\times 10^{-3}$ s, and in the distance between two lasers is less than 1 mm. The experimental techniques described above allow us to obtain "average" information *i.e.* the ball undergoes many collisions (typically for 5 cm, the distance between two successive lasers, the number of collisions is of the order of 50) so the fluctuations are integrated in space and time.

2.3 Video measurements

We have also recorded the ball trajectories by using a video system. A CCD camera is placed above the rough plane far enough from the release point to ensure observing the mean constant velocity regime. The typical field of view is 100 times the diameter of the recorded ball. The camera takes 25 images per second, *i.e.* the time between two successive images δt is fixed and equal to 0.04 s. The smallest average velocity we observed is 6.6 cm/s, and if one assumes roughly one collision per glass bead, as found by Henrique *et al.* [19], we estimate the time between two collisions is $\delta t = 0.015$ s *i.e.* the average number of collisions between two frames is 2.6. The highest average velocity is 12.8 cm/s so $\delta t = 7.81 \times 10^{-3}$ s which corresponds to 5 collisions. This means that each frame gives an average over 3 to 5 collisions. In practice, for each (R, θ) value we launch twenty balls with the same initial velocity. The R values we considered are 1.5 mm, 2 mm and 2.5 mm. The videotapes are visualized image by image and the ball position is determined and noted at each step on a transparent paper placed on a TV screen. For each pair (R, θ), we have recorded the paths of the ball on the transparent paper which is then photocopied and digitized. Each trajectory is saved in a different computer file. The error due to the distortion linked to the photocopier and the scanner do not exceed one percent. The coordinates $(x_{i,j}, y_{i,j})$ of each point of the trajectory are obtained by computing the barycenters using the image analysis software NIH. This procedure may seem tedious but the direct processing of data using image processing software is exceedingly difficult due to multiple light reflections from glass beads constituting the surface and the weak contrast between the steel ball and the plane. We can compute for each (R, θ) pair and for a given trajectory the local velocity components $\mathbf{v}_{x_{i,j}}$ and $\mathbf{v}_{y_{i,j}}$, the modulus of the local velocity $\mid \mathbf{v}_{i,j} \mid$ and the angle $\alpha_{i,j}$ between the direction of the total velocity and the x-direction. So

$$v_{x_{i,j}} = \frac{x_{i,j} - x_{i-1,j}}{\delta t}, \tag{2}$$

$$v_{y_{i,j}} = \frac{y_{i,j} - y_{i-1,j}}{\delta t}, \tag{3}$$

$$\mid v_{i,j} \mid = \sqrt{v_{x_{i,j}}^2 + v_{y_{i,j}}^2}, \tag{4}$$

$$\alpha_{i,j} = arctan \frac{v_{y_{i,j}}}{v_{x_{i,j}}}, \tag{5}$$

where j labels the trajectory and i labels the coordinates for successive δt for a given trajectory.

The mean values $\overline{V_x}$, $\overline{V_y}$ and $\overline{\mid V \mid}$ are calculated for each R and θ from the local velocities by averaging over the twenty recorded trajectories as follows:

$$\overline{V_x} = \frac{1}{N} \sum_{j,i} v_{x_{i,j}}, \tag{6}$$

$$\overline{V_y} = \frac{1}{N} \sum_{j,i} v_{y_{i,j}}, \tag{7}$$

$$\overline{\mid V \mid} = \frac{1}{N} \sum_{j,i} \sqrt{v_{x_{i,j}}^2 + v_{y_{i,j}}^2}, \tag{8}$$

where N is the total number of velocities summed over all the trajectories and is different for each (R, θ) value.

3 Experimental results

3.1 Velocities and angles

In this section, we examine the velocities obtained as explained above. In Figure 2 we show $\overline{V_x}$ and $\overline{\mid V \mid}$ as functions of $\sin(\theta)$ for $R = 2.5$ mm.

We see that both $\overline{V_x}$ and $\overline{\mid V \mid}$ vary linearly with $\sin(\theta)$, and the same behaviour is observed for the other ball sizes.

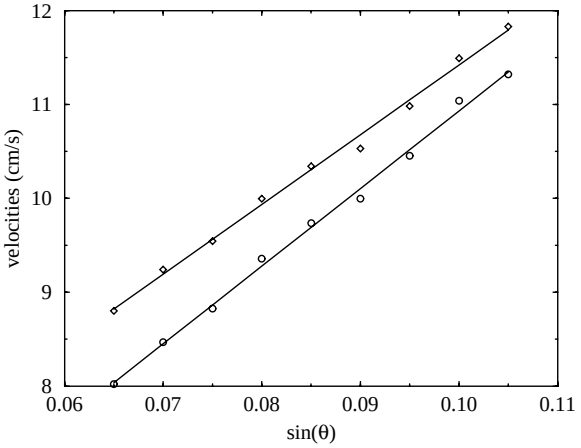

Fig. 2. The mean velocity $\overline{V_x}$ ($\circ$) and the total mean velocity ($\diamond$)$\overline{\mid V \mid}$ for $R = 2.5$ mm as a function of θ.

This behaviour of $\overline{V_x}$ is in agreement with that found previously (see Sect. 1). The average velocity can, therefore, be expressed as:

$$\frac{\overline{V_x}}{\sqrt{rg}} R^{-1.25} = D + C\sin(\theta). \qquad (9)$$

Clearly as $\theta \to 0$, $\overline{V_x}$ does not go to zero. The reason for that is clear. Recall that the mean constant velocity regime is defined for θ values between two transition zones (A)–(B) and (B)–(C). For a given value of R (or $\Phi = R/r$) the lower limit of region (B) is given by θ_{AB}, the transition angle to the pinning regime (A): for $\theta < \theta_{AB}$ the ball stops. Therefore, we cannot ask the question of what happens to $\overline{V_x}$ as θ goes to zero. The constant, D, in equation (9) has no physical meaning.

The fact that $\overline{V_x}$ grows linearly with $\sin(\theta)$ means that the velocity dependent component of the friction force depends linearly on the velocity. This friction force, due to collisions, is therefore viscous. Finally, let us add that in those experiments the exponent β from the scaling of the mean velocity with R was found equal to 1.25, which we write explicitly in equation (9).

Looking now at $\overline{\mid V \mid}$ we see that it is obviously larger than $\overline{V_x}$ whatever angle θ is considered, but it increases more slowly with $\sin(\theta)$. This can be explained by the fact that the values of the local $v_{y_{i,j}}$ slightly decrease (as will be shown in Fig. 5), while the local $v_{x_{i,j}}$ increase, as the inclination of the rough plane goes up. So the relative importance of $v_{y_{i,j}}$ decreases as θ increases.

The trajectory recordings give the components of the local velocities in the direction of the mean flow $v_{x_{i,j}}$ and perpendicularly $v_{y_{i,j}}$. In Figure 3, $v_{x_{i,j}}$ is displayed as a function of $v_{y_{i,j}}$, for two inclination angles of the rough surface.

In Figure 3a we see clearly that for small values of θ, *i.e.* close to the transition between the regime (A) and (B) of the phase diagram, strong correlations appear between the two components. In case (a), when $v_{x_{i,j}}$ is close to zero,

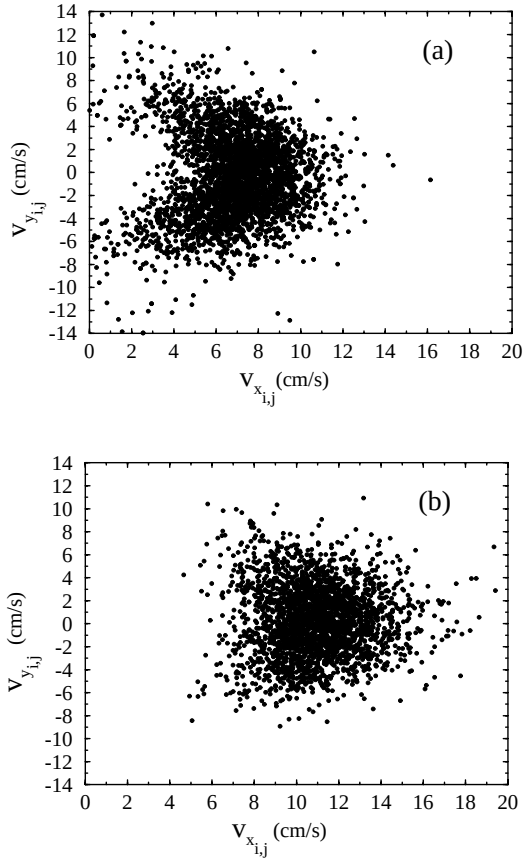

Fig. 3. The local velocity $v_{x_{i,j}}$ as a function of the component $v_{y_{i,j}}$ for $R = 2.5$ mm and (a) $\theta = 3.15^\circ$ (shows strong correlations), (b) $\theta = 5.6^\circ$ (shows little correlations).

$\mid v_{y_{i,j}} \mid$ takes large values, which corresponds to values of $\alpha_{i,j}$ close to ± 90 degrees as will be seen below, *i.e.* the ball deviates completely from the mean flow direction. For such angles, we cannot consider separately the x and y direction. As θ increases, the $v_{x_{i,j}}$ values are shifted towards higher values, as seen in Figure 3b. The $v_{x_{i,j}}$ and $v_{y_{i,j}}$ are no longer preferentially distributed, and we do not observe correlations between the components of the x and y local velocities. In consequence, the x and y direction can be treated separately.

Figure 4 shows the histogram corresponding to the velocity fluctuations for the tranverse speed $v_{y_{i,j}}$.

Such a distribution can be well fitted by a Gaussian. We obtain similar distributions for other (R, θ) values in the mean constant velocity regime, except for the smallest θ-values. We will see below that for such small inclination angles, the motion of the ball is qualitatively different. From these distributions we can compute the mean square deviations $\overline{\Delta V_y{}^2}$, which are shown in Figure 5.

We observe that the transverse velocity fluctuations $\overline{\Delta V_y{}^2}$ decrease as the inclination of the rough surface increases. For a given inclination, the velocity fluctuations perpendicular to the mean flow are close whatever is the

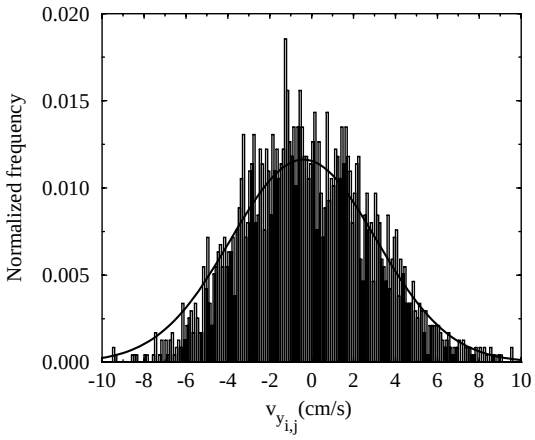

Fig. 4. Histogram of the fluctuations of the transverse velocity, $v_{y_{i,j}}$, for $R = 2.5$ mm and $\theta = 4.9°$.

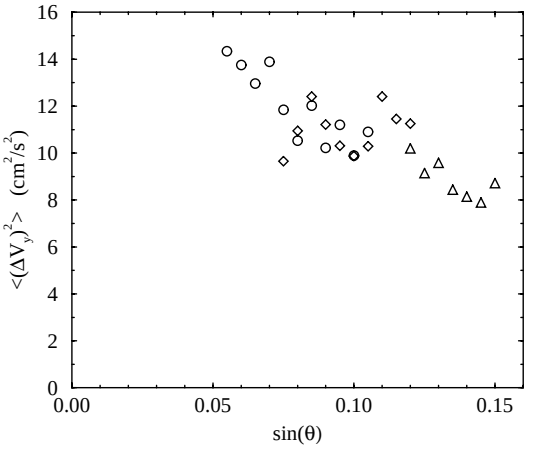

Fig. 5. Mean square deviations $\langle(\Delta V_y)^2\rangle$ as a function of $\sin(\theta)$ for $R = 1.5$ mm ($\triangle$), $R = 2$ mm ($\diamond$) and $R = 2.5$ mm ($\circ$).

size of the moving particle. These results could be linked to those of transverse diffusion (see below).

Another way of studying the motion is to investigate the angular fluctuations. Using the local velocities $v_{x_{i,j}}$ and $v_{y_{i,j}}$ we have analysed the distributions of the angles of deviation $\alpha_{i,j}$ defined above as the angle between $\mathbf{v}_{i,j}$ and $\mathbf{v}_{x_{i,j}}$. This study was done for each pair (R and θ) and over twenty trajectories. Figure 6 shows typical distributions of the deviation angle.

All the experimental distributions were found to be fitted well by Gaussians, when the angles θ considered are far from the transition between the regime (A) and (B), as in Figure 6b. However, it can be seen in Figure 6a that for small θ, *i.e.* very close to the A–B transition of the phase diagram two little bumps are localized at $-90°$ and $90°$ which means that the ball may deviate completely from the x direction. This observation is in agreement with the results found from the velocity correlations (in Fig. 3a).

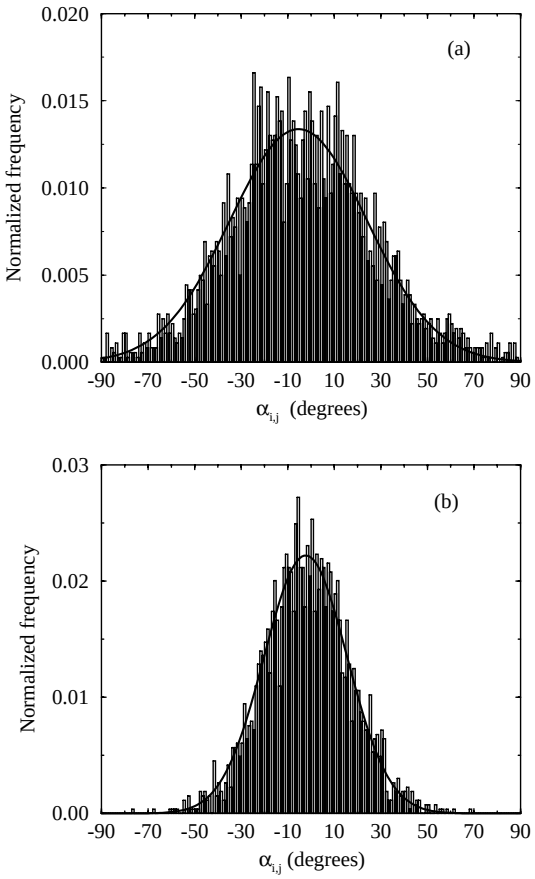

Fig. 6. Typical distributions for the angles $\alpha_{i,j} = \arctan(v_{y_{i,j}}/v_{x_{i,j}})$ for $R = 2.5$ mm, (a) $\theta = 2.6°$ and (b) $\theta = 4.9°$.

3.2 Transverse dispersion

In order to analyse the transverse dispersion for a given θ, R, and L, we count the balls in each bin of the collector for each of the three release points and we sum the counts for these three experiments. We compare all the distributions obtained for R, θ and L by computing the mean square deviations $\overline{\Delta y^2}$ of the Gaussian distribution. In order to do so, we plot the cumulated frequencies on a galtonian paper versus the number of bins, *i.e.* the abscissa. The width of the distribution for given values of R, θ, L is not exactly the same depending on the position where the balls are released. Nevertheless we have verified that this difference is weak and does not exceed three percent in an experiment performed on 3600 launched balls. For given R and θ values, L is increased from 80 cm to 170 cm in steps of 15 cm. $\overline{\Delta y^2}$ is found to increase linearly to L

$$\overline{\Delta y^2} = a_{(R,\,\theta)} L \tag{10}$$

which is shown in Figure 7. If V_0 is much higher than $\overline{V_x}$ the moving ball has to experience a longer transient dynamics before reaching the steady state regime and an additive constant appears in equation (10), which depends

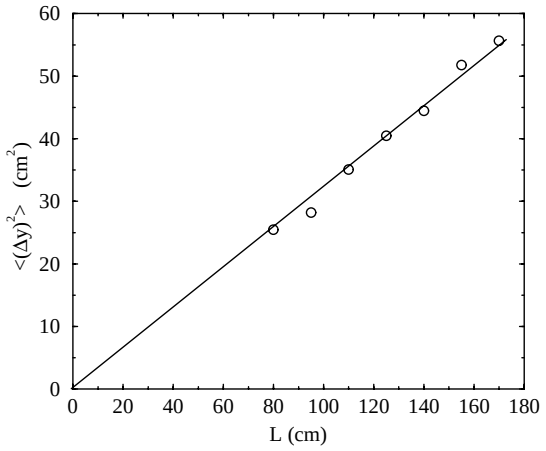

Fig. 7. Variation of the mean square deviation, $\overline{\Delta y^2}$, with L for $R = 3$ mm and $\theta = 4^\circ$.

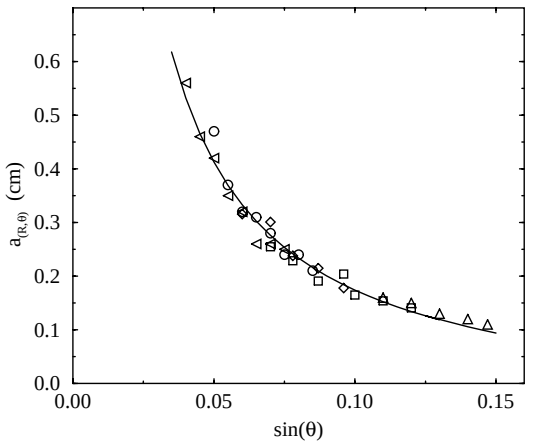

Fig. 8. Variation $a_{(R,\,\theta)}$ as a function of $\sin(\theta)$ for $R = 1.5$ mm ($\triangle$), $R = 2$ mm ($\square$), $R = 2.5$ mm ($\diamond$), $R = 3$ mm ($\circ$), $R = 3.5$ mm ($\triangleleft$).

on the initial velocity V_0. Nevertheless the slope $a_{(R,\,\theta)}$, which characterizes the dispersion is not affected. The only way to modify or introduce another effect on the dispersion is to change the direction of the initial velocity of the ball which in the present study was carefully controlled. In our experiments V_0 is chosen always close to $\overline{V_x}$ for a given couple (R, θ) values, which implies that the equation (10) is always verified.

Equation (10) indicates that the moving balls have a diffusive behaviour in the direction perpendicular to the mean flow. These experiments were performed in the regime (B), characterized by a constant velocity, *i.e.* the mean transit time $\overline{t_c}$ grows linearly with the travelled distance L. So equation (10) corresponds to a diffusive behaviour analogous to a classic random walk as for brownian motion. It can be seen that in our case, the diffusion is not due to thermal agitation because of the size of the moving particles. From Figure 8 it can be clearly seen that all the data fall on the same curve, *i.e.* $a_{(R,\,\theta)}$ does not depend on the radius, R, of the moving ball, at least for the sizes of the particles studied.

Moreover $a_{(R,\,\theta)}$ decreases as $\sin(\theta)$ goes up. In fact this curve is an hyperbola, *i.e.* $a_{(R,\,\theta)}$ can be written as a function of $1/\sin(\theta)$:

$$a_{(R,\,\theta)} = \frac{A}{\sin(\theta)} + B. \tag{11}$$

In our experiments the fit gives respectively for A and B, 0.024 cm and -0.065 cm. The length $a_{(R,\,\theta)}$ can be regarded as the characteristic length scale, *i.e.* the velocity correlation length of the system. As seen in Figure 8, $a_{(R,\,\theta)}$ ranges from about 0.1 cm for large θ to about 0.6 cm for small θ (close to the diameter of the largest steel balls used in the figure, 0.7 cm). The small characteristic length corresponding to large angles is of the same order as the size of the beads on the surface. this can be understood from experiments [19] and numerical simulations [16] that show that for large angles, the moving ball travels on average one bead diameter between two collisions. The fluctuations in the velocity (direction and magnitude) are due to these collisions and, for larger inclinations, the velocity of the ball is large enough, that it can bounce on and over the tops of the surface beads on its way down the plane. Thus, these collisions induce uncorrelated fluctuations in the x and y velocities (see Fig. 3b). On the other hand, when θ decreases, the characteristic length goes up. The nature of the motion is modified: the ball follows paths that offer low potential barriers, *i.e.* the valleys formed on the surface. These low potential barriers are not only due to the geometry, but to a combination of the geometry and the energy the moving ball. In this region, the characteristic length scale in Figure 8 becomes larger than the rough surface bead size and is closer to the moving ball size. In this case the velocity correlation length becomes of the same order as the rolling ball size. It seems that for this range of angles the ball travels the rough plane by rolling rather than bouncing. Dippel *et al.* [16] have shown numerically that rotation should not be neglected at small inclination angles. At the moment, this effect cannot be studied experimentally. In addition, numerical simulations [20], taking into account only the geometry, have shown the important role played by it in such systems. Moreover, in these simulations, the same value of $a_{(R,\,\theta)}$ for a given θ is found for different values of R. When θ becomes very small, *i.e.* close to the transition between the regions (A) and (B), the motion is not truly diffusive since, for example, when the x velocity goes down, it is because the ball made a turn to follow the valley and, consequently, the y velocity goes up (see Fig. 3a and the discussion in the following section).

Let us consider now the coefficient of diffusion D_y of this random walk and the influence of the rolling ball size and the inclination angle of the surface. Equation (10) may be rewritten:

$$\overline{\Delta y^2} = 2D_y\overline{t_c}, \tag{12}$$

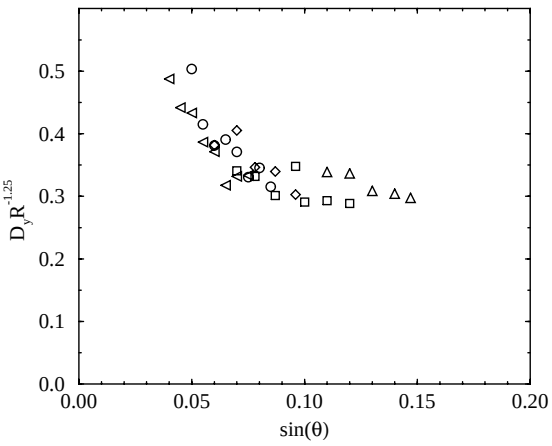

Fig. 9. The scaled coefficient of transverse diffusion as a function of $\sin(\theta)$, obtained by the collector $R = 1.5$ mm ($\triangle$), $R = 2$ mm (square), $R = 2.5$ mm ($\diamond$), $R = 3$ mm ($\circ$), $R = 3.5$ mm ($\triangleleft$).

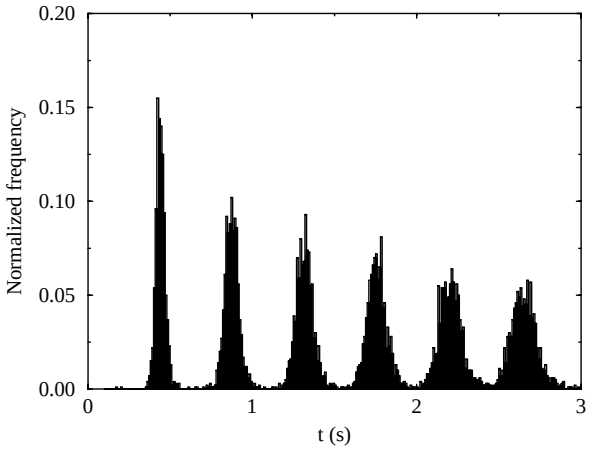

Fig. 10. Transit time distributions at the different laser positions for $R = 3$ mm and $\theta = 4.6°$.

where $\overline{t_c}$ is the mean time needed to travel the distance L. Therefore

$$\overline{\Delta y^2} = 2D_y \frac{L}{\overline{V_x}}, \tag{13}$$

and

$$D_y = \frac{\overline{V_x}}{2}\frac{\overline{\Delta y^2}}{L} = \frac{\overline{V_x}}{2} a_{(R,\,\theta)}. \tag{14}$$

For a given ball size, we find that the transverse coefficient of diffusion decreases as θ goes up. Moreover, this decrease is greater with increasing values of R. We found that all the data for the different R values collapse on the same curve if we scale D_y by $R^{-1.25}$ for the range of inclination angles studied. This is shown in Figure 9. This dependence of D_y on $\sin(\theta)$ can be very easily understood by substituting equations (9, 11) in equation (14).

Another way to calculate the transverse coefficient of diffusion is to do it from the velocity fluctuations as for a particle falling in a fluid in which there is a given concentration of particles [21]. This method can be used for the transverse diffusion as well as for the longitudinal diffusion. The velocity fluctuations are obtained from the trajectory recordings. Unfortunately, these trajectories are not long enough to have a sufficiently good statistics. Nevertheless the coefficients of diffusion obtained by this way are of the same order of magnitude as those presented here.

3.3 Longitudinal dispersion

By analogy with studies on fluid flows in porous media, the tracer dispersion process can be described by a convection-diffusion equation [22]:

$$\frac{\partial c(\mathbf{x},t)}{\partial t} + (\mathbf{v}\cdot\boldsymbol{\nabla})c(\mathbf{x},t) = D_{\parallel}\Delta_{\parallel}c(\mathbf{x},t) + D_{\perp}\Delta_{\perp}c(\mathbf{x},t) \tag{15}$$

where $c(\mathbf{x},t)$ is the tracer concentration at a given position $\mathbf{x}$, at time t, with a mean velocity $\mathbf{v}$. $\Delta_{\parallel}$ and $\Delta_{\perp}$ are respectively the gradients in the parallel direction to the mean velocity and perpendicular to it. $D_{\parallel}$ and $D_{\perp}$ are respectively the longitudinal and the tranverse coefficients of diffusion. In porous media, these coefficients are closely linked to the disordered structure of the velocity field in the pores space and permit to characterize the media. This equation is observed in several situations and we consider the case of the asymptotic behaviour predicted by the central limit theory. When the mean flow is in one direction, dispersion in the transverse direction can be neglected in comparison to the longitudinal one and equation (15) is then one-dimensional. In the case of the rough plane, such a simplification cannot be made. The time fluctuations are sufficiently small for a given abscissa in comparison with the mean transit time between two consecutive measurement abscissae. This is verified for most of the (R, θ) couples under consideration. For each pair (R, θ) we measure and record the transit time between the laser beams for each particle all in region (B). The timer is triggered by the first laser x_0 (*cf.* Fig. 1) placed just at the exit of the launcher but at this point the ball has not yet reached its stationary state. The second laser x_1, chosen as the reference, is placed far enough down the plane to ensure that the ball has achieved its constant average velocity. The transit time distributions obtained at the different laser positions x_i are displayed in Figure 10. These distributions are very well fitted by Gaussians. Nevertheless when the inclination angle of the rough surface becomes small enough for a given R, a tail at long time appears. This tail is longer the smaller θ gets. To begin with, we will focus on the cases of θ and R for which the tail of the distribution may be neglected. We have computed the corresponding first and second moments of the particle transit time distribution $\overline{t}$ and $\overline{\Delta t^2} = \overline{t^2} - \overline{t}^2$. The first moment is used to calculate the constant mean velocity, while the second moment characterizes the particle dispersion. $\overline{\Delta t^2}$ is related

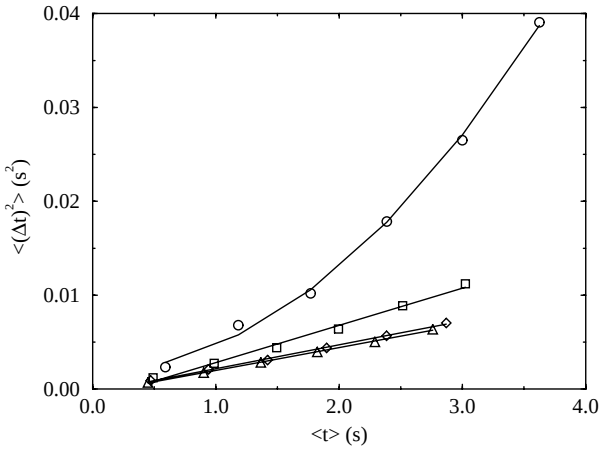

Fig. 11. Variation of the mean square deviation of the transit time of the ball on the rough surface with the mean transit time for $R = 3$ mm, and $\theta = 2.9°$ (○), $\theta = 3.75°$ (square), $\theta = 4°$ (◇), $\theta = 4.3°$ (△).

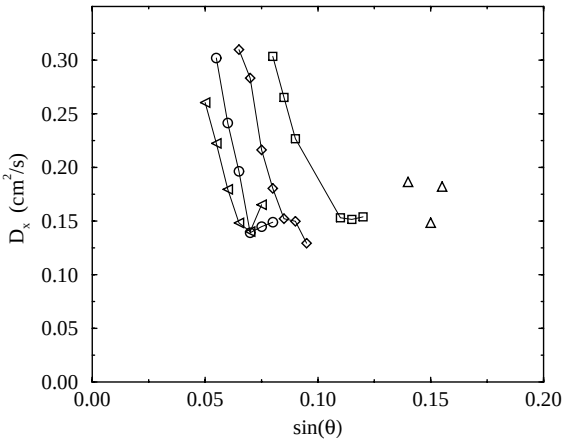

Fig. 12. Variation of the longitudinal dispersion coefficient D_x as function of the mean velocity $\sin(\theta)$ by the laser measurements: $R = 1.5$ mm (△), $R = 2$ mm (square), $R = 2.5$ mm, (◇), $R = 3$ mm (○), $R = 3.5$ mm (◁).

to the longitudinal dispersion coefficient D_x by [23]:

$$D_x = \frac{\overline{V_x}^2}{2} \frac{\overline{\Delta t^2}}{\overline{t}} \cdot \tag{16}$$

In Figure 11, $\overline{\Delta t^2}$ is displayed as a function of $\overline{t}$ obtained from the gaussian fit for $R = 3$ mm and for several inclination angles. We see that the linear variation predicted by equation (16) is well satisfied for sufficiently large angles θ and corresponds to diffusive behaviour. It can be noticed that $\overline{\Delta t^2}$ decreases while the inclination angle goes up, for a given mean transit time $\overline{t}$.

On the other hand, at small angles we observe deviations from linear behaviour (*cf.* Fig. 11 for $\theta = 2.9°$). These deviations occur for the same angles where we have found strong correlations between the x and y components of the velocities and emphasize the presence of another type of behaviour. This behaviour can be explained by the velocity correlations (in Fig. 3a) caused by the fact that the ball follows valleys of low potential energy barriers, as discussed in the previous section. This departure of $\overline{(\Delta t)^2}$ from linearity indicates that at small angles of inclination the motion is not diffusive. This being the case for the longitudinal case, it must also be true for transverse motion. We could not have verified this using the video measurements because we lacked the high statistics needed.

For most values of R and θ, the behaviour was found to be diffusive and the corresponding local velocities in the x and y directions were decorrelated. Using equation (16) we determine the diffusion coefficient, D_x, which is shown in Figure 12 as a function of the inclination angle θ for all R values studied. For all values of R, we see that as θ increases D_x approaches the limiting value 0.15 cm^2/s. The angle at which this value is reached depends on R but the limiting value of D_x does not. A possible explanation of this is as follows. As θ is increased, the velocity of the ball increases, and bouncing becomes the dominant mode of motion and the typical length is governed in this case by the mean separation between grains of the surface. When bouncing dominates, the ball sees mainly the tops of the beads on the surface with which it collides regardless of R. Since the nature of these collisions is the same for all R (since they all take place at the top of the beads) they lead to the same values for D_x.

As for the case of transverse diffusion, one could define a longitudinal characteristic length l_d which is the ratio of D_x over $\overline{V_x}$. From the values of D_x and $\overline{V_x}$ we see that l_d is smaller than 1 mm (0.1 mm $< l_d <$ 0.4 mm). That is the longitudinal length is smaller than the smallest typical length of the system which is the typical distance between the glass beads constituting the rough surface. So l_d seems not to be the actual characteristic length. We are unable to explain physically why l_d takes such small values. Nevertheless the comparison with the transverse diffusion shows that the longitudinal length is much smaller than the transverse one. This is opposite to what is observed in porous media: transverse dispersion is neglected compared to the longitudinal one, and is imposed by the mean flow. In addition, when the porous medium is homogeneous and unconsolidated, the characteristic length is found to be of the order of magnitude of the bead sizes. In this sense, the ball motion in a rough surface shows a surprising behaviour where anisotropy is not determined by the direction of the mean velocity.

4 Discussions and conclusions

Dispersion measurements in fluid flow in porous media are an important tool for obtaining information about length scales that characterize the geometrical heterogeneities of the medium. The dispersion coefficients are very sensitive to the velocity fluctuations linked to the random geometry.

The dispersion measurements we carried out on the rough plane gave similar interesting information. We

found for the motion of the ball on the rough plane in regime (B) that the ball has two different behaviours: for a given R and for θ large enough, the motion is *diffusive* and the characteristic length is of the order of 1 mm (the mean size of the bumps on the surface), showing that it is governed by the geometry of the surface. In this regime, the fluctuations in the x and y components of the velocity are independent and are caused by the random collisions between the moving ball and the surface bumps. The main mechanism for energy dissipation, therefore, appears to be collisional.

However, for small θ, *i.e.* close to the transition between the pinning zone (regime (A)) and the constant velocity one (regime (B)), this diffusive character seems to disappear. Instead, we find that there are very strong correlations between the fluctuations of the x velocity and those of the y velocity. This is due to the fact that for small velocities, *i.e.* small θ, the ball mostly follows valleys of smallest potential barriers. Thus the x and y motions are strongly correlated and the diffusive behaviour vanishes. Here the characteristic length increases up to values of the sizes of the rolling ball.

Molecular dynamics simulations of a sphere moving down an inclined plane consisting of similar spheres of smaller size [15,16] have been performed. From these simulations, the motion of the particles was studied in detail.

These simulations yield results that are in very good qualitative and quantitative agreement with the experiments. The main difference between the two is due to uncertainties in the coefficients restitution needed in the simulations. This seems to cause numerical simulations to give a region (B) which is a little narrower than the experimental results. The simulations found the motion to be diffusive both in the transverse and longitudinal directions with values similar to the experimental ones. In particular, D_x and D_y were found to behave differently, just as in our experiments. A similar anisotropy is found in porous media or in sedimentation, but the diffusion coefficient corresponding to the mean direction velocity motion is larger than the one corresponding to the transverse direction [24]. In our cases, the reverse is true.

We wish to thank D. Bideau, A. Calvo, S. Dippel, C. Henrique and J.P. Hulin for very fruitful discussions. We thank also S. Bourles, P. Chasle and B. Truffin for conceiving the experimental setup. This work was supported by the GdR CNRS "Physique des Milieux Hétérogènes Complexes".

References

1. J.C. Williams, Chem. Proc. Sup., April 1965.
2. A. Rosato, K. Istrandburg, F. Prinz, R.H. Swendsen, Phys. Rev. Lett. **58**, 1038-1040 (1987).
3. R. Jullien, P. Meakin, A. Pavlovitch, Phys. Rev. Lett. **69**, 640-643 (1992).
4. J. Duran, J. Rajchenbach, E. Clement, Phys. Rev. Lett. **70**, 2431-2434 (1993).
5. M.H. Cooke, J. Bridgwater, Ing. Eng. Fundam. **18**, 25-27 (1979).
6. S.B. Savage, *Developments in Engineering Mechanics, edited by A.P.S. Selvadurai* (Elsevier, Amsterdam, 1987) p. 347.
7. S.B. Savage, C.K K. Lun., J. Fluid. Mech. **180**, 311-335 (1988).
8. F.X. Riguidel, A. Hansen, D. Bideau, Europhys. Lett. **28**, 13-18 (1994).
9. F.X. Riguidel, R. Jullien, G. Ristow, A. Hansen, D. Bideau, J. Phys. I France **4**, 261-272 (1994).
10. M.A. Aguirre, I. Ippolito, A. Calvo, C. Henrique, D. Bideau, Powd. Tech. **94**, 85-89 (1997).
11. L. Samson, Ph.D. thesis, Université de Rennes I (1997).
12. R.A. Bagnold, Proc. Roy. Soc. Lond. A **225**, 49-63 (1954).
13. R.A. Bagnold, Proc. Roy. Soc. Lond. A **295**, 219-232 (1966).
14. G.G. Batrouni, S. Dippel, L. Samson, Phys. Rev. E **53**, 6496-6503 (1996).
15. S. Dippel, G.G. Batrouni, D.E. Wolf, *HLRZ Workshop on Friction, Arching, Contact Dynamics* (World Scientific, Singapore 1997).
16. S. Dippel, G.G. Batrouni, D.E. Wolf, Phys. Rev. E **56**, 3645-3656 (1997).
17. The lasers emit at 620 nm and the power is 4mW.
18. The phototransistor BPY62 has a sensibility of 850 nm and the spectrum is ranged between 420 nm and 1130 nm.
19. C. Henrique, M.A. Aguirre, A. Calvo, I. Ippolito, G.G. Batrouni, D. Bideau, Powd. Tech. **92**, 75-80 (1997).
20. J. Lemaitre, L. Samson, L. Oger, P. Richard, *Foams, emulsions and cellular materials*, edited by N. Rivier (Kluwer Acad. Publishers Dordrecht, 1997) (to appear).
21. H. Nicolai, B. Herzhaft, E.J. Hinch, L. Oger, E. Guazzelli, Phys. Fluids **7**, 12-22 (1995).
22. J. Bear, *Dynamics of fluids in porous media* (Elsevier Publishing Co., New York, 1972).
23. J. Koplik, *Disorder and Mixing*, edited by E. Guyon, J.P. Nadal, Y. Pomeau (Kluwer Acad. Publishers Dordrecht, 1987) pp. 123-137.
24. W. Kalthoff, S. Schwarzer, G. Ristow, H. Herrmann, Int. J. Mod. Phys. C **7**, 543-561 (1996).